High-Pressure Studies as a Novel Approach in Determining Inclusion Mechanisms: Thermodynamics and Kinetics of the Host−Guest Interactions for α-Cyclodextrin Complexes

Amira Abou-Hamdan,* Pascal Bugnon, Christophe Saudan, Peter G. Lye, and André E. Merbach*

Contribution from the Institut de Chimie Minérale et Analytique (ICMA), Université de Lausanne, Bâtiment de Chimie (BCH), CH-1015 Lausanne, Switzerland

Received August 30, 1999. Revised Manuscript Received November 8, 1999

Abstract: The first volume profiles for complex formation of α-cyclodextrins (α-CD) with diphenyl azo dyes (S) are presented as a new approach in understanding inclusion phenomena. The following dyes were selected: sodium 4-(4-diethylaminophenylazo)benzenesulfonate (**1**), sodium 4-(3-carboxy-4-hydroxy-5-methylphenylazo)benzenesulfonate (**2**), sodium 4-(4-hydroxy-3,5-dimethylphenylazo)benzenesulfonate (**3**), and sodium 2-hydroxy-3-methyl-5-(4-sulfamoylphenylazo)benzoate (**4**). The behavior of the dyes alone were first studied in aqueous solutions to rule out any competition reaction. Under the experimental conditions used for the stopped-flow kinetic studies, it has been proved that only monomeric species are present (no aggregation of the dye is formed by $\pi-\pi$ stacking interactions). NMR experiments and kinetic evidences have shown that only directional binding of the dye via the sulfonate/sulfonamide group through the wide rim of the α-cyclodextrin was possible. The 1:1 complex was the only stoichiometric species formed. The inclusion reactions for the four selected dyes were characterized by a two-step kinetics described by a first fast step that yields the intermediate, S·α-CD*, followed by a slower rearrangement to form the final complex, S·α-CD. 2D NMR experiments served for a molecular dynamics calculation leading to a structural representation of the intermediate and final complexes. An interpretation of the volume profiles obtained from high-pressure stopped-flow kinetic experiments have not only confirmed the so far proposed mechanisms based on "classical" kinetic investigations but offered a new focus on the inclusion process. The inclusion mechanism can be summarized now as follows: the complexation begins with an encounter of the dye and α-cyclodextrin mainly due to hydrophobic interactions followed by a partial desolvation of the entering head of the dye. The latter interacts with the two "activated" inner water molecules of the free host and their complete release is delayed by the primary hydroxy group barrier of the α-CD. At this first transition state, a squeezed arrangement develops inside the cavity inducing a negative activation volume ($\Delta V_{1,f}^{\ddagger} \approx -8$ to -24 cm^3 mol^{-1}). The subsequent intermediate is characterized by a total release of the two inner water molecules and interactions of the dye head with the primary hydroxy groups of the host in a trapped-like structure ($\Delta V_1^{\circ} \approx -11$ to -4 cm^3 mol^{-1}). The latter interactions and concurrent tail interactions with the secondary hydroxy groups of the host lead at different extents to a strained conformation of the host in the second transition state ($\Delta V_{2,f}^{\ddagger} \approx -2$ to -16 cm^3 mol^{-1}). In the final complex, the head of the dye is totally rehydrated as it protrudes from the primary end of the host cavity which can now adopt a released conformation ($\Delta V_2^{\circ} \approx +3$ to $+6$ cm^3 mol^{-1} vs $+17$ cm^3 mol^{-1} for **1**).

Introduction

Cyclodextrins (CD) are well-known in supramolecular chemistry as molecular hosts capable of including with a degree of selectivity a range of guest molecules via noncovalent interactions in their hydrophobic cavity. These cyclic oligomers of α-D-glucose are described as a shallow truncated cone, the primary hydroxy rim of the cavity opening having a reduced diameter compared to the secondary hydroxy rim. Much attention was given in recent years[1] to these supramolecular complexes of cycloamyloses due to their significance, through the understanding of the noncovalent binding forces, for the development of

enzyme analogues[2] and their industrial importance, particularly with respect to drug encapsulation and targeting. Despite the wealth of interest in inclusion complexes of α-cyclodextrin, there has been relatively few kinetic studies and of these none have involved high-pressure kinetic measurements. In fact, most kinetic studies dealing with inclusion reactions involving

(1) (a) Easton, C. J.; Lincoln, S. F. *Modified Cyclodextrins*; Imperial College Press: London, 1999. (b) Szejtli, J. *Chem. Rev.* **1998**, *98*, 1743. (c) Hedges, A. R. *Chem. Rev.* **1998**, *98*, 2035. (d) Uekama, K.; Hirayama, F.; Irie, T. *Chem. Rev.* **1998**, *98*, 2045. (e) Li, S.; Purdy, W. C. *Chem. Rev.* **1992**, *92*, 1457. (f) Amato, M. E.; Pappalardo, G. C.; Perly, B. *Magn. Reson. Chem.* **1993**, *31*, 455. (g) Lipkowitz, K. B. *Chem. Rev.* **1998**, *98*, 1829.

(2) Bender, M. L.; Komiyama, M. *Cyclodextrin Chemistry*; Springer-Verlag: Berlin, 1978.

(3) (a) Cramer, F.; Saenger, W.; Spatz, H.-Ch. *J. Am. Chem. Soc.* **1967**, *89*, 14. (b) Hersey, A.; Robinson, B. H. *J. Chem. Soc., Perkin Trans. 1* **1984**, *80*, 2039. (c) Seiyama, A.; Yoshida, N.; Fujimoto, M. *Chem. Lett.* **1985**, 1013. (d) Örstan, A.; Wojcik, J. F. *Carbohydr. Res.* **1985**, *143*, 43. (e) Yoshida, N.; Fujimoto, M. *J. Phys. Chem.* **1987**, *91*, 6691. (f) Clarke, R. J.; Coates, J. H.; Lincoln, S. F. *Adv. Carbohydr. Chem. Biochem.* **1988**, *46*, 205. (g) Yoshida, N.; Seiyama, A.; Fujimoto, M. *Adv. Carbohydr. Chem. Biochem.* **1990**, *94*, 4246 and 4254. (h) Yoshida, N.; Hayashi, K. *J. Chem. Soc., Perkin Trans. 2* **1994**, 1285 and references therein. (i) Yoshida, N.; Fujita, Y. *J. Phys. Chem.*. **1995**, *99*, 3671.

α-cyclodextrin (α-CD) have been carried out at atmospheric pressure using temperature or the chemical composition of the medium as experimental variables.[3] The interpretation of the results of such experiments is sometimes not simple since the change of temperature produces simultaneous changes both in volume and thermal energy, and their effects are difficult to separate.[4a] In contrast, using pressure as the experimental variable allows one to perturb in a controlled manner only the volume of the system (density) under study keeping the thermal energy constant.[4] Preliminary high-pressure work[5] dealing with complex formation of α-cyclodextrin with anions and cations yielded molar volume changes without so far solid interpretation of the data. On the other hand, no activation volumes determined from the pressure dependence of the rate constants have been reported to date. In the field of inorganic chemistry, kinetic studies at different pressures of substitution reactions, for example, have been extensively applied in a few laboratories and enabled mechanistic discriminations of basic importance.[4,6] Among other aspects, this success of high-pressure studies is related to the fact that it is comparatively simple to interpret volume differences in molecular terms even in the case of complex chemical systems whereas it is often very difficult to interpret enthalpy and entropy differences on a similar level.

The cyclodextrins have stimulated many discussions on the subject of the forces involved in inclusion complex formation. Few theories were put forth to explain the origins of the cyclodextrin complex stability.[7] The responsible forces were attributed, solely or in combination, to hydrophobic interaction,[7] the relief of cyclodextrin strain energy,[8] release of partially hydrogen-bonded "activated" water molecules from the cavity,[9] London dispersion forces, and dipole−induced dipole interactions.[10] Thus, one can see that cyclodextrin binding, like protein binding, is a complex phenomenon in which noncovalent molecular forces must be reconciled with conformational considerations for a strong and specific binding to occur.

A novel approach is undertaken to determine energetic and geometry features of the inclusion process in aqueous solution of a serie of diphenyl azo dyes (Figure 1) in α-CD and in an effort to further elucidate the complex mechanisms involved in the inclusion reactions of cyclodextrins. It consists of a variable-pressure kinetic study together with the classical variable-temperature investigation coupled to structural NMR and molecular dynamics. The guest molecules were selected in a way to systematically tune steric and electronic effects toward the molecular recognition by the host.

Experimental Section

Materials. The azo guest molecules **1** and **2** were purchased from Aldrich. The azo-dyes **3** and **4** were synthesized via the azo coupling method.[11] The ethylorange **1** was used without further purification whereas **2**, **3**, and **4** were purified by column chromatography as

	R_3	R_4	R_5	Y
1	H	N(Et)_2	H	SO_3^-
2	Me	OH	COO^-	SO_3^-
3	Me	OH	Me	SO_3^-
4	Me	OH	COO^-	SO_2NH_2

Figure 1. Molecular structures (pH ca. 6.5) of the diphenyl azo dyes.

described elsewhere.[3f] α-CD purchased from Fluka was used without further purification. Both the dyes and α-CD were dissolved in doubly distilled water.

Spectrophotometric Measurements. The acid dissociation constants, K_a, of the dyes were determined combining potentiometric and spectrophotometric techniques. The instrumentation used consists of a titroprocessor (Titrino 716 from Metrohm), for the addition of titrant and mV readings, and of a diode array spectrometer (TIDAS-MMS-UV/500-1 from J&M) coupled to an Hellma immersion probe (10 mm path length) for the spectrophotometric measurements. A combined glass electrode (Metrohm) was calibrated from titrations of HCl with NaOH under the same conditions (298 K, $I = 0.15$ M (NaCl)). Thus the pH values are defined as $-\log[H^+]$. The aqueous solutions of the dyes **1** and **2** (($2.5-5) \times 10^{-5}$ M, acidified with HCl and CH_3COOH) were titrated with NaOH 0.1 M at 298 ± 0.1 K, whereas the aqueous solution of the dyes **3** and **4** (5×10^{-5} M, basified with NaOH and Na_3PO_4) were titrated with HCl 0.1 M. The ionic strength, I, was fixed to 0.15 M with NaCl. The solutions were thoroughly mixed and allowed to equilibrate before the spectrum was acquired directly with the immersion probe present inside the titration vessel. The pK_a values of the dyes were calculated using the Global Analysis[12] software SPECFIT.[13]

The dye self-association ($\pi-\pi$ stacking) has been determined by spectrophotometric and NMR (vide infra) techniques. For the spectrophotometric measurements, the dye concentration was varied between 8.3×10^{-3} and 2.5×10^{-7} M. The spectra were recorded at 298 K with a Perkin-Elmer Lambda19 spectrophotometer, adapting the optical path length between 1 and 10 cm to the dye concentration.

The stability constants of the inclusion complexes of α-CD with the dyes were determined at 298 K from spectrophotometric titrations using the same instrumentation described above for the acid dissociation constants determination. Aqueous solution of each dye (2.8×10^{-5} M) was titrated with α-CD (3.8×10^{-4} M) whereupon starting with a large excess of the dye, the α-CD to dye ratio reached 10 at the end of the titration. The ionic strength is assumed to be zero, as the only charged species originate from the dyes which are at a maximum concentration of 5×10^{-5} M. The stability constant K_T for binding of each dye to α-CD was determined from the spectral changes using the multiwavelength Global Analysis[12] software SPECFIT.[13]

Kinetic Measurements. Both the dye [$(2.5-5) \times 10^{-5}$ M] and uncharged α-CD [$(0.3-5) \times 10^{-3}$ M] were dissolved in doubly distilled water without the addition of an electrolyte. The kinetics of the inclusion reaction between the dye and α-CD has been investigated by the

(4) (a) Winter, R.; Jonas, J., Eds. *High-Pressure Chemistry, Biochemistry and Materials Science*; Kluwer Academic Publishers: Dordrecht, 1993. (b) Isaacs, N. S., Ed. *High-Pressure Food Science, Bioscience and Chemistry*; Royal Society of Chemistry: Letchworth, UK, 1998.

(5) Høiland, H.; Hald, L. H.; Kvammen, O. J. *J. Solution Chem.* **1981**, *10*, 775.
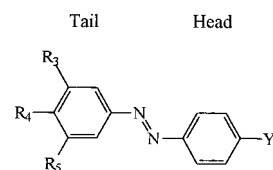
(6) Lincoln, S. F.; Merbach, A. E. *Adv. Inorg. Chem.* **1995**, *42*, 1. van Eldik, R.; Hubbard, C. D., Eds. *Chemistry Under Extreme or Non-Classical Conditions*; John Wiley & Sons and Spektrum Akademischer Verlag: USA, 1997. Asano, T.; Le Noble, W. J. *Chem. Rev.* **1978**, *78* (4), 407. Drljaca, A.; Hubbard, C. D.; van Eldik, R.; Asano, T.; Basilevsky, M. V.; Le Noble, W. J. *Chem. Rev.* **1998**, *98,* 2167.

(7) Connors, K. A. *Chem. Rev.* **1997**, *97*, 1325.

(8) Manor, P. C.; Saenger, W. *J. Am. Chem. Soc.* **1974**, *96*, 3690.

(9) Griffiths, D. W.; Bender, M. L. *Adv. Catal.* **1973**, *23*, 209.

(10) Bergeron, R. J.; Channing, M. A.; Gibeily, G. J.; Pillor, D. M. *J. Am. Chem. Soc.* **1977**, *99*, 5146.

(11) Vogel, A. I. *Practical Organic Chemistry*; Longman Group Limited: London, 1974; p 624.

(12) (a) Gampp, H.; Maeder, M.; Meyer, C. J.; Zuberbühler, A. D. *Talanta* **1985**, *32*, 95. (b) Gampp, H.; Maeder, M.; Meyer, C. J.; Zuberbühler, A. D. *Talanta* **1985**, *32*, 257. (c) Gampp, H.; Maeder, M.; Meyer, C. J.; Zuberbühler, A. D. *Talanta* **1985**, *32*, 1133. (d) Gampp, H.; Maeder, M.; Meyer, C. J.; Zuberbühler, A. D. *Talanta* **1986**, *33*, 943.

(13) SPECFIT 2.11 for MS-DOS, Spectrum Software Associates, P.O. Box 4494, Chapel Hill, NC 27515, U.S.A., e-mail: *SpecSoft@compuserve.com*.

(14) (a) Dye **1**: $T = 276, 287, 298, 308,$ and 320 K, between 300 and 600 nm each 15 nm. (b) Dye **2**: $T = 278, 288, 298, 308,$ and 318 K, between 300 and 600 nm each 15 nm. (c) Dye **3**: $T = 278, 288, 298, 308,$ and 318 K, between 300 and 600 nm each 15 nm. (a) Dye **4**: $T = 274, 278, 283,$ and 288 K, between 300 and 600 nm each 15 nm.

Table 1. Acid Dissociation Constants (pK_a) of the Dyes at 298 K, $I = 0.15$ M

1	2	3	4
4.11 ± 0.01 (HN(Et)$_2^+$/N(Et)$_2$)	2.46 ± 0.02 (COOH/COO$^-$) 11.88 ± 0.01 (OH/O$^-$)	8.07 ± 0.04 (OH/O$^-$)	2.25 ± 0.13 (COOH/COO$^-$) 10.15 ± 0.12 (SO$_2$NH$_2$/SO$_2$NH$^-$) 12.06 ± 0.01 (OH/O$^-$)

stopped-flow technique under pseudo-first-order conditions in the presence of at least a 10-fold excess of α-CD.

Temperature-dependent kinetic measurements were carried out between 274 and 318 K on an Applied Photophysics SX.18MV stopped-flow spectrometer, using the multiple shot facility.[14]

Pressure-dependent kinetic measurements were carried out up to 200 MPa[15] using our high-pressure stopped-flow spectrometer designed and built in house.[16] A J&M TIDAS diode array spectrometer was used for detection when reaction time and absorbance amplitude allowed it. In other cases, the pressure dependence of the reaction was monitored at discrete wavelengths using the mono-wavelength detection system and the acquisition facility provided with the Applied Photophysics SX.18MV stopped-flow spectrometer. For each set of experimental conditions, series of two to four replicate data sets were averaged.

For both the temperature and pressure multiwavelength experiments, the observed rate constants were computed by iterative procedure of the absorbances/time data to exponential functions with global analysis software.[12,13] Reported errors are one standard deviation.

NMR Measurements. ^{1}H NMR experiments were recorded on Bruker ARX 400 (400 MHz), DPX 400 (400 MHz), and AMX2 600 (600 MHz) spectrometers. All NMR experiments (dye titrations by α-CD, differential NOE, dilution experiments, etc.) were carried out in D$_2$O solution at 298 K with the residual HOD as an internal standard. All 2D experiments were recorded with the sample nonspinning. NMR spectroscopic data processing was carried out on a Bruker Silicon Graphics O2 station with standard UXNMR software as well as on a PC using 1D WIN NMR (960901) software (Bruker Franzen Analytik GmbH). The dqf-COSY and ROESY were acquired using 512 increments of 2 K data points and 16 scans each. For ROESY, a CW spin-lock field of 2 kHz was used and spectra were acquired with a 400 ms mixing time. The data were zero-filled twice in the t_1 dimension, and multiplied by a squared sinebell function (SSB 2) in both dimensions. For the NMR spectral measurements, solutions of guests (3.5×10^{-2} M) in D$_2$O (pD ca. 6.5) were titrated with consecutive additions of solid α-CD. The resulting solutions were thoroughly mixed and allowed to equilibrate several minutes before the spectrum was acquired. The value of the bound percent, defined as the percent ratio of the complexed guest to the total guest, varied between 0 and 100%.

Restrained Molecular Dynamics Simulation. Simulations were done on a Silicon Graphics Octane using the program CVFF[17] force field as implemented in Discover (version 97; Molecular Simulations, 1997), starting from structures of α-CD (Cambridge library) and **3** (minimized in Cerius^2 version 3.8, Molecular Simulations, 1998) and including the corrected NOE constraints obtained from the ROESY spectrum.

The molecular dynamics runs were performed using standard Discover protocols at a constant temperature of 300 K, with a distance-dependent dielectric term ($\epsilon = 4.00r$) approximating aqueous surroundings, including charges and an infinite cutoff for nonbonded interactions to partially compensate the lack of the solvent.[18] The initial structure was minimized for 200 steps of steepest descent, followed by a

conjugate gradient minimization until the rms gradient was <0.001 kcal/(mol Å). After 10 ps of initialization time, the system was subjected to a 50 ps simulation time with 0.5 fs time steps. Structures were saved every 0.5 ps. All resulting 100 structures were subjected to the same minimization protocol as described above.

Results

Equilibrium and Structural Aspects. All the equilibrium and kinetic (vide infra) measurements were carried out at pH around 6.5. It was thus essential to study the protonation behavior of the selected dyes and determine the existing species under such a condition. The attribution of the acid dissociation constants, determined from spectrophotometric titrations and summarized in Table 1, is obvious considering the functional groups of these dyes. According to the results, one can assume that the guest molecules in pure water exist predominantly in the forms which are shown in Figure 1. It is noteworthy that some studies have demonstrated that the values of the acid dissociation constants (pK_a) of guest molecules can be enhanced upon inclusion in the cyclodextrins.[19] But in the case of α-cyclodextrin only a negligibly small increase of the pK_a was observed for a series of azodyes[3g] implying that the dyes remain mainly in the forms given in Figure 1. Also in previous studies,[20] an increase in the association constants of guest molecules with α-CD was observed upon addition of electrolytes such as NaCl (ca. 1 M) resulting from increased water structuring by these relatively small and hard ions (salting out effect). Moreover, electrolyte ions are known to form inclusion complexes with cyclodextrins.[21] In this study, such side effects were avoided since the stopped-flow technique, unlike the T-jump method classically used in the CD inclusion studies, did not require the addition of electrolytes.

Turning to the ^{1}H NMR measurements, the full assignment of the chemical shifts of the dyes and α-CD was fulfilled using 2D-COSY, ROESY, and NOEDIF experiments. These values as well as the chemical shift variations of the host and guest upon inclusion of the substrate in the cyclodextrin cavity are given in the Supporting Information deposited with this paper. In fact, being carried out on high magnetic field spectrometers (400 and 600 MHz), the present investigation required the application of spin-lock techniques such as ROESY[22,23] for obtaining sizable NOEs.

The 1D ^{1}H NMR titrations of the guests with α-CD resulted in the appearance of two states (S·α-CD* and S·α-CD) of the inclusion complexes for **1**, **2**, and **3** and only one inclusion complex for **4**. On the other hand, after a closer look at the spectra it became evident that the chemical shifts of the free guest molecules were also very concentration dependent (see the case of dye **3** in Figure 2).

(15) (a) Dye **1**: $T = 308$ K, between 300 and 600 nm each 2 nm. (b) Dye **2**: $T = 288$ K, between 300 and 600 nm each 2 nm. (c) Dye **3**: $T = 288$ K, between 300 and 600 nm each 2 nm. (a) Dye **4**: $T = 278$, K, between 300 and 600 nm each 2 nm.

(16) Bugnon, P.; Laurenczy, G.; Ducommun, Y.; Sauvageat, P.-Y.; Merbach, A. E.; Ith, R.; Tschanz, R.; Doludda, M.; Bergbauer, R.; Grell, E. *Anal. Chem.* **1996**, *68*, 3045.

(17) Hagler, A. T.; Huler, E.; Lifson, S. *J. Am. Chem. Soc.* **1974**, *96*, 5319.

(18) Weiner, S. J.; Kollman, P. A.; Case, D. A.; Singh, U. C.; Ghio, C.; Alagona, G.; Profeta, S.; Weiner, P. J. *J. Am. Chem. Soc.* **1984**, *106*, 765.

(19) Connors, K. A.; Lipari, J. M. *J. Pharm. Sci.* **1976**, *65*, 379.

(20) Schneider, H.-J.; Kramer, R.; Simova, S.; Schneider, U. *J. Am. Chem. Soc.* **1988**, *110*, 6442.

(21) Rohrbach, R. P.; Rodriguez, L. J.; Eyring, E. M.; Wojcik, J. F. *J. Phys. Chem.* **1977**, *81*, 944.

(22) Bothner-By, A. A.; Stephens, R. L.; Lee, J.; Warren, C. D.; Jeanloz, R. W. *J. Am. Chem. Soc.* **1984**, *106*, 811.

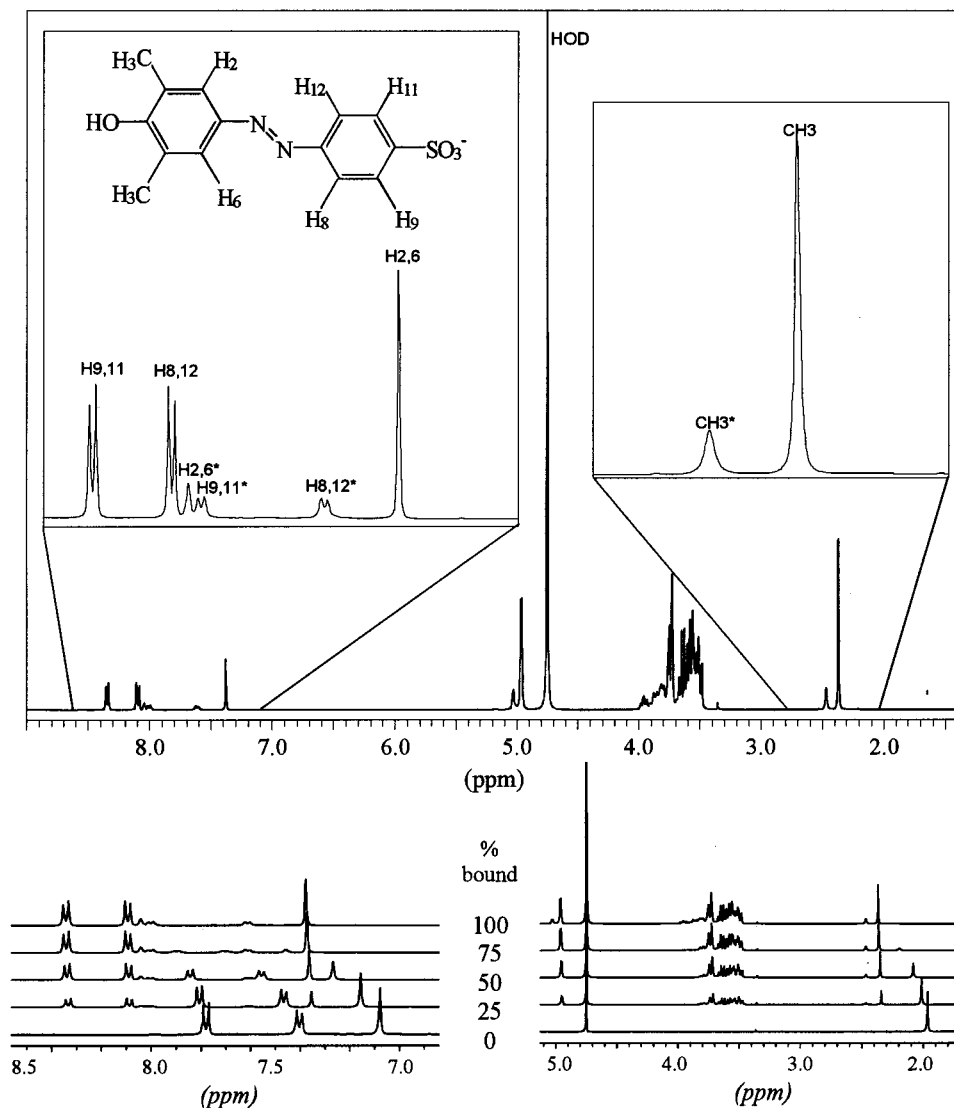(23) Bax, A.; Davis, D. G. *J. Magn. Reson.* **1985**, *63*, 207.

Figure 2. ^{1}H NMR spectra for the titration of **3** with α-CD in D$_2$O at 298 K, pD ca. 7. Bottom: Percent of total bound **3** (**3**·α-CD* and **3**·α-CD) with respect to total **3** concentration of 0.0344 M. Top: Enlargement and labeling of the guest part in the final spectrum; the signals of bound α-CD lie between 3.4 and 4.0 at 5.0 ppm.

To interpret such a variation, we decided to explore the possibility of the self-association of the dyes in D$_2$O:

$$2S \xrightleftharpoons{K_{assoc}} S_2 \qquad (1)$$

Indeed the π−π stacking driven self-association (mainly dimerization since higher order aggregation beyond dimerization is insignificant in the studied concentration range) of the aromatic azo guest molecules is well-known,[24] and this induces chemical shift changes. From the ^{1}H NMR titrations of the dyes with α-CD, the dimerization (eq 1) is a fast process on the NMR time scale since only an average set of signals of the free guest is observed (an example is given in Figure 2). On the contrary, the inclusion process to form the bound species is much slower as indicated by the presence of separate sets of NMR signals, S·α-CD* and S·α-CD, except for dye **4** where only one set of NMR signals is observed.

The chemical shifts of H$_{9,11}$, H$_{8,12}$, H$_{2,6}$, and CH$_3$ of a solution of dye **3** experienced an upfield shift of 0.13, 0.40, 0.63, and

0.26 ppm, respectively, as the concentration of the dye decreased from 80.00 to 3.87 × 10^{-2} mM in D$_2$O.

Upon introduction of the observed chemical shifts for all four sites and the corresponding analytical concentrations, a least-squares fit was performed using eqs 2 and 3 where C is the total concentration of the monomer, yielding a $K_{assoc} = 11 \pm 3$ M^{-1} (see the fits in Supporting Information).

$$K_{assoc} = \frac{[S_2]}{[S]^2} = \frac{[S_2]}{C - 2[S_2]^2} \qquad (2)$$
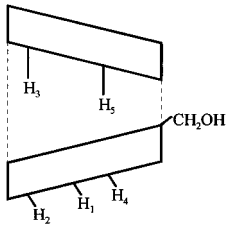
$$\delta_{obs} = \delta_S p_S + \delta_{S_2} p_{S_2} = \delta_S(C - 2[S_2])/C + \delta_{S_2}(2[S_2])/C \qquad (3)$$

Furthermore, when this dilution experiment for **3** was repeated in d_5-pyridine, no concentration-dependent chemical shift changes were observed indicating the absence of dimerization. This reflects the π association with the solvent molecules and further supports a π-driven association of the dye molecules.

Calculations of the ring current induced shifts of dye **3** were carried out using the program provided by Perkins[24a] which is based on the Johnson−Bovey theory.[25] One possible geometry

(24) (a) Perkins, S. J. *Biol. Magn. Reson.* **1982**, *4*, 193. (b) Gerasimowicz, W. V.; Wojcik, J. F. *Bioorg. Chem.* **1982**, *11*, 420. (c) Clarke, R. J.; Coates, J. H.; Lincoln, S. F. *Carbohydr. Res.* **1984**, *127*, 181. (d) Shetty, A. S.; Zhang, J.; Moore, J. S. *J. Am. Chem. Soc.* **1996**, *118*, 1019.

(25) Johnson, C. E., Jr.; Bovey, F. A. *J. Chem. Phys.* **1958**, *29*, 1012.

Table 2.   Experimental Upfield Shift, $\Delta\delta$ Values for the Inner Protons of the α-CD Due to Complex (S·α-CD) Formation[a]

	1	2	3	4
$\Delta\delta$ H$_3$/ppm	−0.245	−0.322	−0.323	−0.371
$\Delta\delta$ H$_5$/ppm	−0.185	−0.246	−0.264	−0.261
$^3J_{1,2}$/Hz	2.75	2.84	3.00	2.62

[a] $^3J_{1,2}$ is the coupling constant in S·α-CD (3.20 Hz for free α-CD).

of the dimeric species that accounts for the experimental chemical shift changes upon dilution is an antiparallel orientation of the two molecules of dye **3** separated by ca. 3.5 Å. Differential NOE experiments confirmed this geometry of dimerization (see Figure S1 in Supporting Information). Similar structural behavior is expected for the other three dyes.

The value of the self-association constant, K_{assoc}, for **3** was confirmed by UV−vis spectrophotometric dilution measurements where a deviation of the linear relationship between concentration and absorbance was noticeable. This proved the presence of more than one form of the free dye molecules in solution. Fitting simultaneously the absorbance values at five different wavelengths as a function of the analytical concentration of the dye gave an association constant of 15 ± 0.2 M^{-1} (see the fits in Supporting Information), thus confirming the value obtained from the NMR data. Now since we are working with analytical dye concentrations of $(2.5-5) \times 10^{-5}$ M for our stability and kinetic studies, the presence of the dimeric species can be thus neglected (dimer coexists with the monomeric form in less than 0.2% of the total dye concentration).

A further analysis of the ^{1}H NMR titration spectra showed for all four complexes that the addition of α-CD to the dye solution caused major upfield shifts of both H$_3$ and H$_5$ protons located inside the host cavity (those of S·α-CD are given in Table 2). This is attributed to the ring current shielding effect[26] of the aromatic portions of the included guests and indicates that the insertion of the guest molecules is quite deep in the cavity of the host. Simultaneously, for all four systems, the free dye exhibits downfield complexation induced shifts. The α-CD complex of dye **3** was selected for molecular modeling calculations using the intermolecular ROEs (corrected for the ROE offset effects[27]) as distance restraints[1g,28] (see Figure 3). Upon a close analysis of the obtained structures for the α-CD complex of **3** using Discover the intermediate and final products seem to be inserted quite deeply in the α-CD cavity as shown in Figure 4. The ensuing discussion will be couched in these findings and focused on offering further proof for the proposed mechanism of inclusion.

Furthermore, no chemical shift changes are detected for the two inclusion species of guests **1**, **2**, and **3** as well as the inclusion complex of **4** as a function of the α-CD concentration.

(26) (a) Yoshida, N. *J. Chem. Soc., Perkin Trans. 2* **1995**, 2249. (b) Rekharsky, M. V.; Goldberg, R. N.; Schwarz, F. P.; Tewari, Y. B.; Ross, P. D.; Yamashoji, Y.; Inoue, Y. *J. Am. Chem. Soc.* **1995**, *34*, 8830. (c) Demarco, P. V.; Thakkar, A. L. *Chem. Commun.* **1970**, 2.
(27) Croasum, W. R.; Carlson, R. M. K. *Two-Dimensional NMR Spectroscopy*; VCH: New York, Weinheim and Cambridge, 1994.
(28) Rüdiger, V.; Eliseev, A.; Simova, S.; Schneider, H−J.; Blandamer, M. J.; Cullis, P. M.; Meyer, A. J. *J. Chem. Soc., Perkin Trans 2* **1996**, 2119.
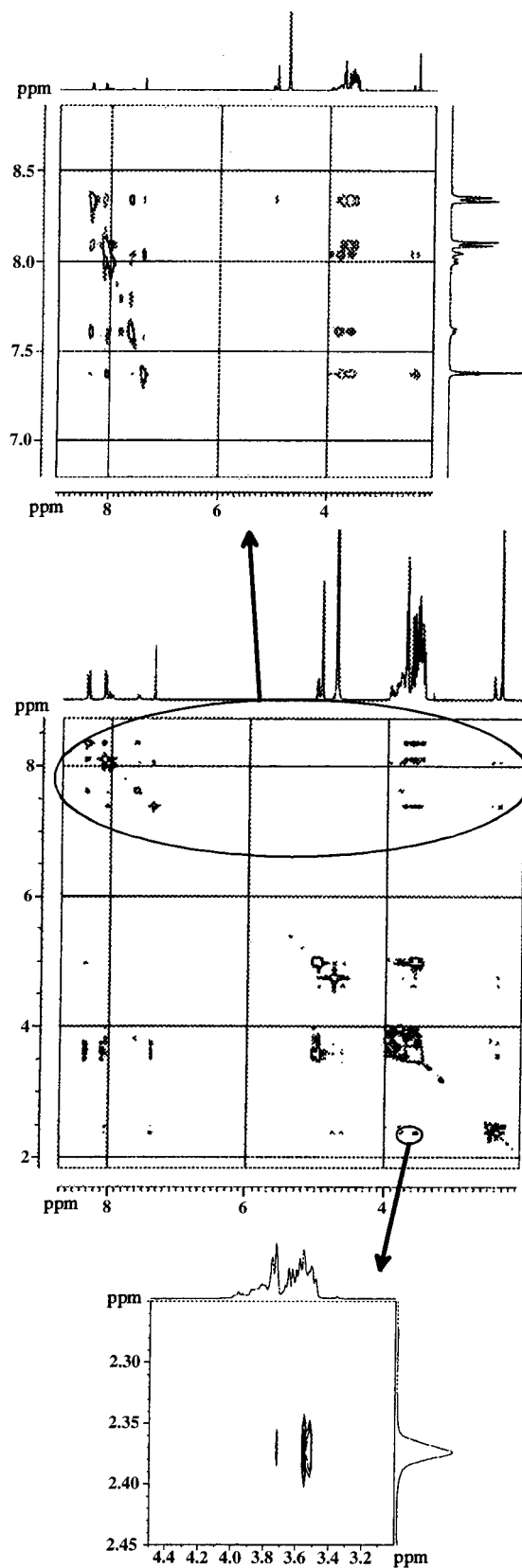
Figure 3. 2D ROESY spectrum of the α-CD complex of **3** in D$_2$O, pD ca. 7, relaxation delay 2 s, spinlock time 400 ms, spinlock field 2 kHz. The upper enlargement shows the intermolecular ROEs of the aromatic part of **3** with the α-CD, whereas the lower enlargement shows that of the methyl group of **3**·α-CD.

The two complexes exist in the constant ratio, K_2^{298} (eq 4), of 2.6, 11.6, and 3.3 for the dyes **1**, **2**, and **3**, respectively (Table

Host−Guest Interactions for α-Cyclodextrin Complexes

J. Am. Chem. Soc., Vol. 122, No. 4, 2000 597

3·α-CD*

3·α-CD

Figure 4. Force field (CVFF) energy minimized structures of intermediate **3·α-CD*** and final product **3·α-CD**. All the hydrogen atoms are omitted for clarity.
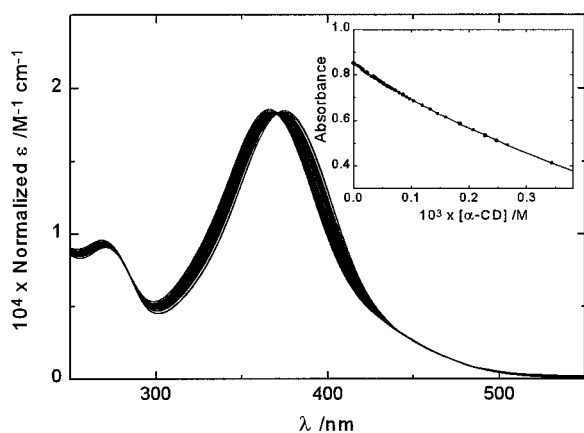
Figure 5. Variation of guest **4** spectrum upon addition of α-CD at 288 K. The insert shows the absorbance at 350 nm to clarify the spectral changes with an increased concentration of α-CD.

3). These equilibrium constants determined from the ^{1}H NMR titrations agree with those obtained from the kinetic measurements which will be discussed in detail (vide infra).

$$S \cdot \alpha\text{-}CD^* \overset{K_2{}^{298}}{\rightleftharpoons} S \cdot \alpha\text{-}CD \qquad (4)$$

Even though the cyclodextrin protons located outside the cavity show negligible or only trivial chemical shift variations, the H_1 protons of the bound α-CD unfold a change of $^3J_{1,2}$ (Table 2) relative to that of the free α-CD (3.20 Hz). The analysis of these coupling constants for the four systems using a Karplus-type equation[29] reveals an alteration of up to 6° in the dihedral angle between H_1 and H_2. Thus the H_1 protons of the host are good detectors of a conformational distortio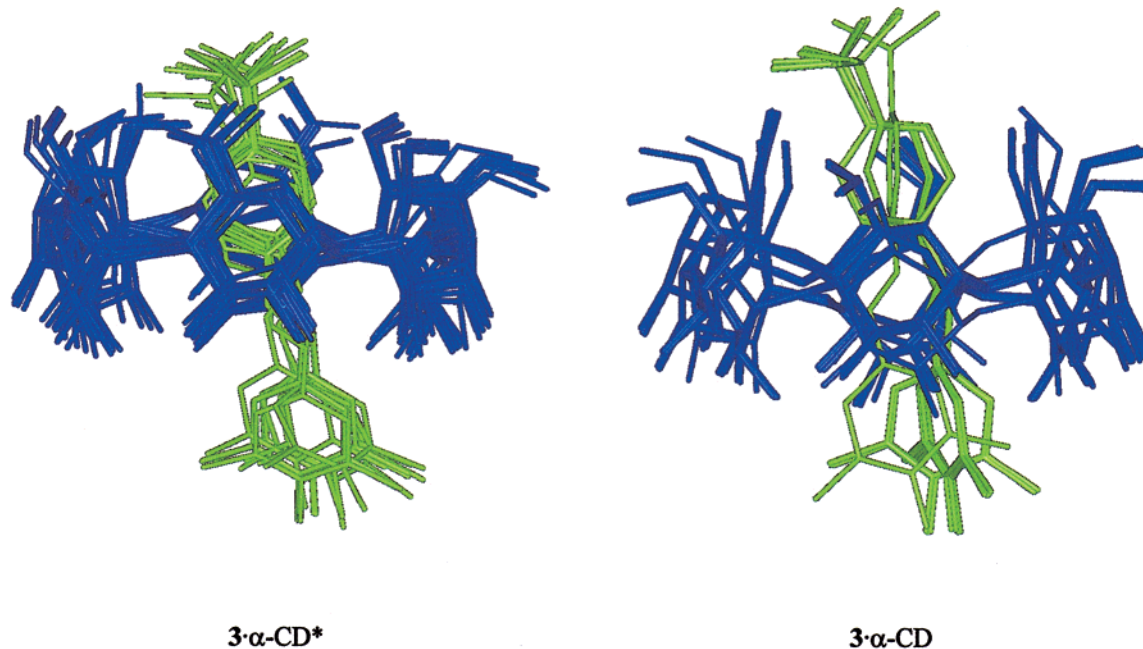n taking place upon the inclusion of the guest molecules. These conformational changes of the host will be further discussed in the context of the mechanistic interpretation.

Turning to the spectrophotometric measurements, an example of the absorbance changes which appear when the substrate

(29) Yamamoto, Y.; Kanda, Y.; Inoue, Y.; Chûjô, R.; Kobayashi, S. *Chem. Lett.* **1988**, 495.
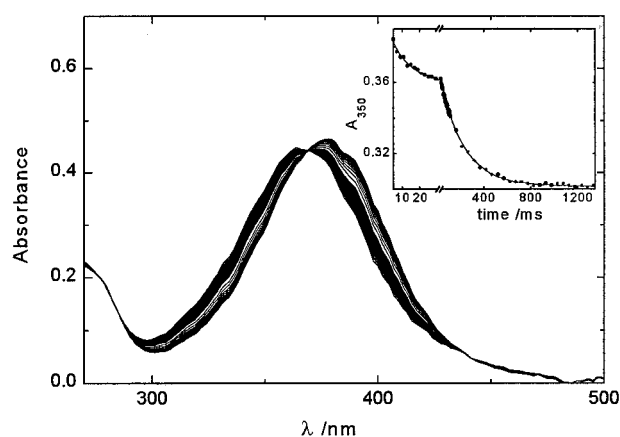
Figure 6. Time-dependent spectra at 100 MPa of the inclusion reaction between guest **4** and α-CD at 278 K. The insert at 350 nm shows measurements over a split time base (total 1st time base 0.030 s and total 2nd time base 1.400 s). $C_{\alpha-CD} = 5.05 \times 10^{-4}$ M, $C_4 = 2.50 \times 10^{-5}$ M, $I = 0$ M.

binds to α-CD is shown in Figure 5 for the titration of a solution of guest **4** by α-cyclodextrin. Only a 1:1 inclusion model (eq 5) fits the optical titration data using the UV−vis spectral changes and the results are given in Table 3.

$$S + \alpha\text{-}CD \overset{K_T}{\rightleftharpoons} S/\alpha\text{-}CD \qquad (5)$$

With $K_T = [S/\alpha - CD]/([S][\alpha - CD])$ and $[S/\alpha\text{-}CD] = [S\cdot\alpha\text{-}CD^*] + [S\cdot\alpha\text{-}CD]$.

A further proof supporting this model came forth from the NMR titration measurements. In fact upon increasing the α-CD concentration up to 12 times that of the dye, no further changes in chemical shifts of the bound substrates occur thus excluding the presence of complexes with different stoichiometries.

Kinetic and Mechanistic Aspects. For all four studied guest molecules two steps are observed for the inclusion process; an example is shown in Figure 6. The observed rate constants for the first fast step, $k_{1,obs}$, show a linear dependence on the α-CD concentration. The values of the observed rate constants of the

Table 3.   Thermodynamic and Kinetic Parameters for the Inclusion Reaction with α-Cd, $I = 0$ M

	1	2	3	4
$k_{1,f}^{298}$/M^{-1} s^{-1}	$(1.22 \pm 0.02) \times 10^4$	$(1.52 \pm 0.03) \times 10^4$	$(1.36 \pm 0.01) \times 10^4$	$(1.67 \pm 0.15) \times 10^5$
$k_{1,r}^{298}$/s^{-1}	1.84 ± 0.1	25.4 ± 0.5	13.3 ± 0.2	380 ± 30
K_1^{298}/M^{-1}	6660 ± 470	600 ± 20	1020 ± 30	440 ± 70
$\Delta H_{1,f}^{\ddagger}$/kJ mol^{-1}	$+20.1 \pm 1$	$+27.3 \pm 1.1$	$+23.0 \pm 0.5$	$+35.1 \pm 3.2$
$\Delta H_{1,r}^{\ddagger}$/kJ mol^{-1}	$+54.8 \pm 3$	$+38.6 \pm 1.2$	$+44.6 \pm 0.9$	$+51.4 \pm 2.9$
ΔH_1^0/kJ mol^{-1}	-34.7 ± 3	-11.3 ± 2.1	-21.6 ± 1.3	-16.4 ± 5.7
$\Delta S_{1,f}^{\ddagger}$/J K^{-1} mol^{-1}	-99.3 ± 3	-73.3 ± 3.8	-88.6 ± 1.7	-27.3 ± 11.6
$\Delta S_{1,r}^{\ddagger}$/J K^{-1} mol^{-1}	-55.9 ± 8	-88.6 ± 4.0	-73.9 ± 2.9	-23.1 ± 10.4
ΔS_1^0/J K^{-1} mol^{-1}	-43.3 ± 10	$+15.2 \pm 7.3$	-14.8 ± 4.2	-4.1 ± 20.4
$k_{2,f}^{298}$/s^{-1}	0.20 ± 0.02	1.83 ± 0.04	0.70 ± 0.02	58 ± 4
$k_{2,r}^{298}$/s^{-1}	$(9.3 \pm 1.2) \times 10^{-2}$	0.17 ± 0.02	0.22 ± 0.01	4.8 ± 0.6
K_2^{298}	2.1 ± 0.5	10.5 ± 1	3.2 ± 0.2	12 ± 2
	2.6^a	11.6^a	3.3^a	
$\Delta H_{2,f}^{\ddagger}$/kJ mol^{-1}	$+72.0 \pm 3$	$+50.8 \pm 1$	$+60.2 \pm 1$	$+58.8 \pm 3$
$\Delta H_{2,r}^{\ddagger}$/kJ mol^{-1}	$+43.8 \pm 3$	$+39.5 \pm 5$	$+47.5 \pm 2$	$+48.3 \pm 5$
ΔH_2^0/kJ mol^{-1}	$+28.2 \pm 5$	$+11.4 \pm 6$	$+12.7 \pm 4$	$+10.5 \pm 6$
$\Delta S_{2,f}^{\ddagger}$/J K^{-1} mol^{-1}	-16.8 ± 9	-69.4 ± 4	-46.0 ± 4	-14.1 ± 10
$\Delta S_{2,r}^{\ddagger}$/J K^{-1} mol^{-1}	-117.7 ± 11	-127.0 ± 17	-98.3 ± 8	-69.9 ± 18
ΔS_2^0/J K^{-1} mol^{-1}	$+100.9 \pm 17$	$+57.6 \pm 19$	$+52.3 \pm 12$	$+55.8 \pm 20$
$\log(K_T^{298}$/M$^{-1})^b$	4.3	3.8	3.6	3.8
	4.18 ± 0.16^c	3.62 ± 0.01^c	3.76 ± 0.03^c	3.65 ± 0.04^c

^{a} Results from NMR titrations. ^{b} $K_T = K_1 + K_1 K_2$. ^{c} Results from spectrophotometric titrations.

Figure 7. Temperature dependence of $k_{1,obs}$ and $k_{2,obs}$, for the inclusion reaction of guest **3** with α-CD: $C_3 = 2.5 \times 10^{-5}$ M, $I = 0$ M, $T = 278$ (■), 288 (●), 298 (▲), 308 (▼), and 318 (◆) K.

Figure 8. Pressure dependence of $k_{1,obs}$ and $k_{2,obs}$, for the inclusion reaction of guest **3** with α-CD: $C_3 = 2.5 \times 10^{-5}$ M, $I = 0$ M, $T = 288$ K, $P = 2$ (■), 50 (●), 100 (▲), 150 (▼), and 200 (◆) MPa.

second slower step, $k_{2,obs}$, increase as a function of the α-CD concentration but reach a saturation value at high α-CD concentration (see Figure 7). It is noteworthy that only the second step of the inclusion reaction of **2** in α-CD was previously detected by Hersey and Robinson.[3b] Moreover the rate and equilibrium constants of the inclusion study of **3** in α-CD were determined by Yoshida and Hayashi[3h] in the presence of electrolytes (0.1 M ionic strength and in the presence of phosphate buffer (pH 4.2−4.5)).

Such biphasic kinetics suggest that a reaction scheme of the type given in eq 6 is required to explain the experimental observations.

If the first step is very fast compared to the second step in eq 6, and if $C_{\alpha-CD}$ (the total α-CD concentration) $\gg C_S$ (the total guest concentration), the observed rate constants can be expressed by eqs 7 and 8, where $K_1 = k_{1,f}/k_{1,r}$.

$$k_{1,obs}(\text{fast}) = k_{1,f} C_{\alpha-CD} + k_{1,r} \tag{7}$$

$$k_{2,obs}(\text{slow}) = k_{2,f}\frac{K_1 C_{\alpha-CD}}{(1 + K_1 C_{\alpha-CD})} + k_{2,r} \tag{8}$$

The $k_{1,obs}$ and $k_{2,obs}$ values obtained at various temperatures were simultaneously analyzed using eqs 7−9. An eight-

$$\text{S} + \alpha\text{-CD} \underset{k_{1,r}}{\overset{k_{1,f}}{\rightleftharpoons}} \text{S·}\alpha\text{-CD*} \underset{k_{2,r}}{\overset{k_{2,f}}{\rightleftharpoons}} \text{S·}\alpha\text{-CD} \tag{6}$$

$$\text{fast} \qquad\qquad \text{slow}$$

$$k = \frac{k_B T}{h}\exp\left(\frac{\Delta S^{\ddagger}}{R} - \frac{\Delta H^{\ddagger}}{RT}\right) \tag{9}$$

$$S + \alpha\text{-CD} \longrightarrow \{S + \alpha\text{-CD*}\}^{\ddagger} \longrightarrow S.\alpha\text{-CD*} \longrightarrow \{S.\alpha\text{-CD}\}^{\ddagger} \longrightarrow S.\alpha\text{-CD}$$
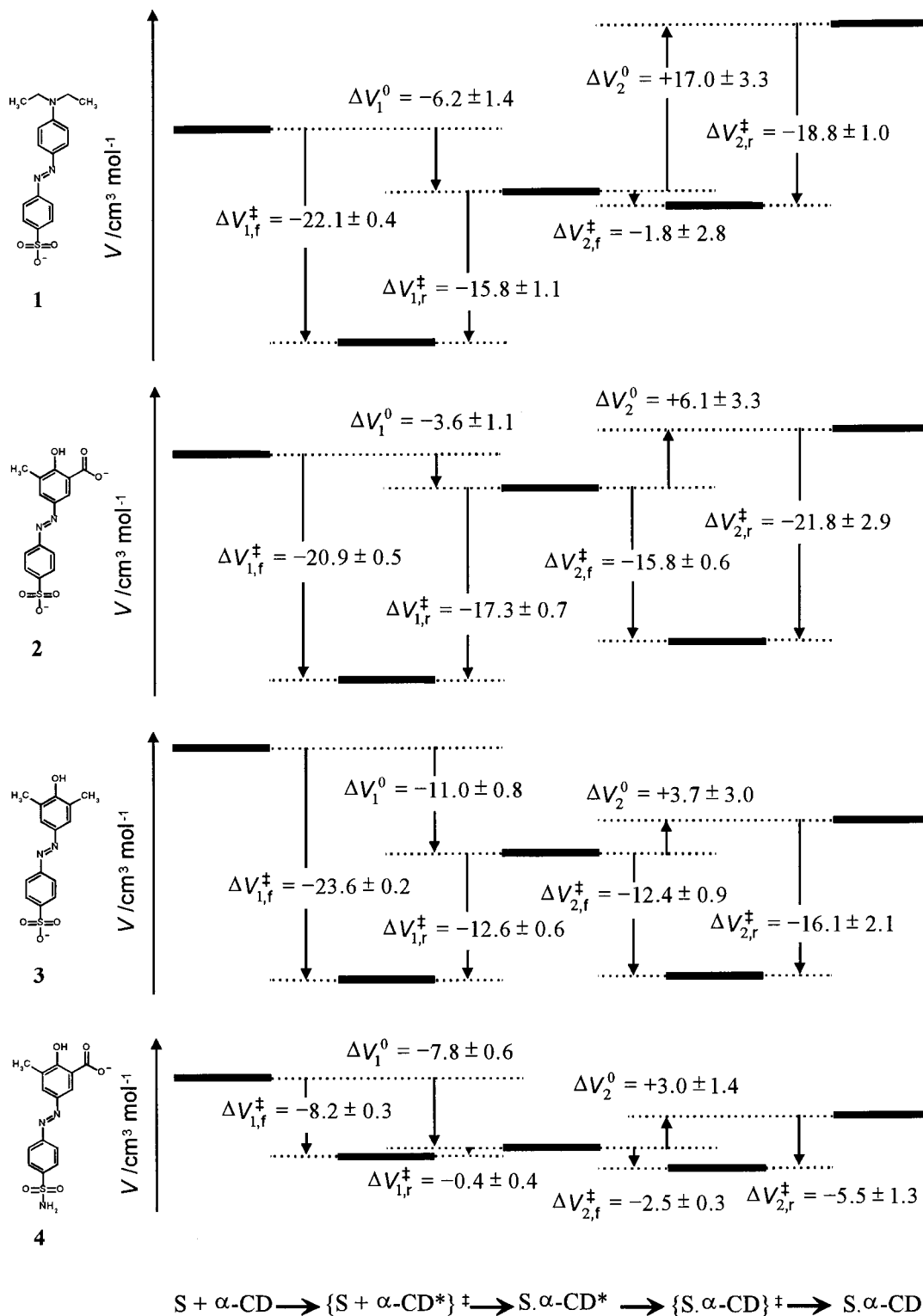
Figure 9. Volume profiles for the inclusion reactions of the four guest molecules (**1** at 308 K, **2** and **3** at 288 K, and **4** at 278 K) with α-CD, in aqueous solutions.

parameter simultaneous analysis of the data (with a weight of the type $1/y^2$) yielded the $\Delta S_{1,f}^{\ddagger}$ (or $k_{1,f}^{298}$), $\Delta S_{1,r}^{\ddagger}$ (or $k_{1,r}^{298}$), $\Delta S_{2,f}^{\ddagger}$ (or $k_{2,f}^{298}$), $\Delta S_{1,r}^{\ddagger}$ (or $k_{2,r}^{298}$), $\Delta H_{1,f}^{\ddagger}$, $\Delta H_{1,r}^{\ddagger}$, $\Delta H_{2,f}^{\ddagger}$, and $\Delta H_{2,r}^{\ddagger}$ values listed in Table 3. The corresponding thermodynamic parameters K_1^{298}, K_2^{298}, ΔH_1^0, ΔH_2^0, ΔS_1^0, and ΔS_2^0 were obtained by replacing $k_{1,r}^{298}$ by $K_1^{298}/k_{1,f}^{298}$, $k_{2,r}^{298}$ by $K_2^{298}/k_{2,f}^{298}$, $\Delta H_{1,r}^{\ddagger}$ by $\Delta H_{1,f}^{\ddagger} - \Delta H_1^0$, $\Delta H_{2,r}^{\ddagger}$ by $\Delta H_{2,f}^{\ddagger} - \Delta H_2^0$, $\Delta S_{1,r}^{\ddagger}$ by $\Delta S_{1,f}^{\ddagger} - \Delta S_1^0$, and $\Delta S_{2,r}^{\ddagger}$ by $\Delta S_{2,f}^{\ddagger} - \Delta S_2^0$. As an example of variable-temperature dependence, Figure 7 shows the results for

the inclusion reaction of dye **3**. The stability constants K_T previously determined by spectrophotometric titrations are also consistent with the reaction presented by eq 6. K_T is, however, a composite one and equal to $(K_1 + K_1 K_2)$.[3b] Good agreement is obtained between kinetic and equilibrium determinations of K_T (see Table 3). The stability constants K_2 calculated from the kinetic experiments are also in good agreement with the NMR determination of the final equilibrium (see Table 3).

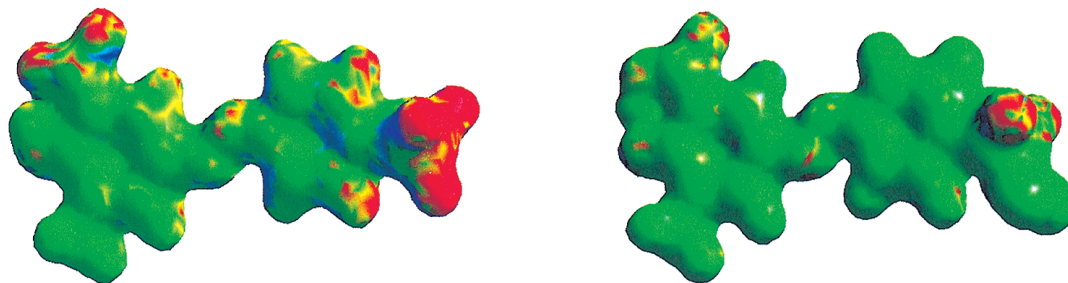The pressure kinetics dependence was determined up to 200

Figure 10. Connolly surfaces of **3** (left) and **4** (right) colored according to the MEP value (G98-HF SCF calculations using the 6-31G* basis set). The lowest (negative) values correspond to the red zone.

MPa. The $k_{1,\mathrm{obs}}$ and $k_{2,\mathrm{obs}}$ values were fitted simultaneously to eq 10 , where k_0 is the rate constant at zero pressure, and $\Delta V^{\ddagger}$

$$ k = k_0 \exp\left(-\frac{\Delta V^{\ddagger} P}{RT}\right) \tag{10} $$

the activation volume. ΔV_1^0 was obtained by replacing $\Delta V_{1,\mathrm{r}}^{\ddagger}$ by $\Delta V_{1,\mathrm{f}}^{\ddagger} - \Delta V_1^0$ and ΔV_2^0 by replacing $\Delta V_{2,\mathrm{r}}^{\ddagger}$ by $\Delta V_{2,\mathrm{f}}^{\ddagger} - \Delta V_2^0$. The errors quoted are 1 standard deviation, but it is clear that, due to nonrandom errors, volumes of activation can only be determined to within 1 cm³ mol⁻¹. The results are shown in Figure 9 and an example of the α-CD complex of **3** is shown in Figure 8.

Discussion

The Inclusion Reaction. Prior to interpreting the thermodynamic and kinetic data, it is essential to confirm (a) the form of the guest species involved in the inclusion reactions and (b) the direction of the guest insertion.

At pH ca. 6.5, the azo guests **1, 3,** and **4** exist as a monovalent anion and **2** as a divalent anion (see Table 1). Despite the fact that dimerization of the dyes (or even higher association) exist via $\pi-\pi$ stacking self-association, the contribution of the dimeric species S_2 of the dye can be neglected under our experimental conditions (vide supra).

The rate, mechanism, and direction of the inclusion into the α-CD cavity are strongly dependent on steric (size and shape) and electronic properties of the host molecules.[3a,h] In our study, a preferential and directional binding of the hydrophilic phenyl ring substituted with the sulfonate/sulfonamide group was clearly concluded. The following points are solicited in favor of such a conclusion: (a) A previous work[3b] reported that the dye 4-(3-methylsalicylateazo),3,5-dimethylbenzene does not bind to α-CD. This was interpreted in terms of steric considerations where both the 3,5-dimethylbenzene species and the 3-methylsalicylate species are too large to be incorporated into the cavity. Therefore, also dyes **2** and **4** can only be inserted via the sulfonate/sulfonamide phenyl ring. (b) Similarly, based on the same work, dye **3** which has a dimethylphenol end, can only be inserted via the sulfonate phenyl ring. (c) The rate at which dye **1** enters the cavity is similar to those of dyes **2** and **3** where the only common structural feature among the three is the sulfonate phenyl ring. On the other hand, it is known[3b] that the insertion rate of Methylorange (which only differs from **1** by its para substitution, $R_4 = N(Me)_2$) in α-CD is much faster than that of **1** and that the insertion takes place via the dimethylamino phenyl entity. It can be thus concluded that dye **1** with its bulkier diethylamino phenyl group (confirmed by molecular modeling) cannot be inserted in a similar way but has to enter the α-CD cavity via the sulfonate phenyl ring.

On the host side, the dye is likely to insert at the more open side of the conical cyclodextrin cavity not only from steric considerations,[7] but also for electronic reasons. The wide rim of the torus is distinctly hydrophilic while the narrow rim bearing the primary hydroxy groups is intensely hydrophobic.[1g] Such mode of insertion is supported by irrefutable evidence from the ROESY spectra, indicating the presence of cross-peaks between the H_2 protons of the host (peripheral protons at the large rim, see Table 2) and the methyl protons of the dimethylphenol of guest **3** in 3·α-CD (see Figure 3) as well as those of the methyl salicylate parts of guests **2** and **4** and the CH_2s of guest **l**.

In conclusion, only insertion of the dye from the sulfonate/sulfonamide group through the wide rim of the α-CD cavity is possible for all four guest molecules.

First Fast Step of the Inclusion. As previously observed,[3h] the overall 1:1 equilibrium constants K_T for our series of azo-dyes of similar skeletal structure are little influenced by changes in the guest substituents (Table 3). On the other hand, kinetic parameters are strongly dependent on steric and electronic effects.[3h,30] The order in $k_{1,\mathrm{f}}$ is as follows: **1** $(-SO_3^-) \approx$ **3** $(-SO_3^-) \approx$ **2** $(-SO_3^-) <$ **4** $(-SO_2NH_2)$. These results suggest that the hydration structure at the periphery of the anionic substituent $-SO_3^-$ may be significant in determining slower rates of insertion and release for the inclusion reaction. This is supported by an observed close van der Waals contact between the inner wall of α-CD and the $-SO_3^-$ group.[3h] From electronic density calculations[31] (Figure 10), it is also obvious that the sulfonate group should be more hydrated than the sulfonamide entity. Even if the order in $k_{1,\mathrm{r}}$ is similar to that of $k_{1,\mathrm{f}}$, the release rate $k_{1,\mathrm{r}}$ is directly dependent on the structure of the non-inserting group of the dye molecule.[30] The less bulky dye **1**, which is only substituted in the para position, is characterized by the smallest release rate $k_{1,\mathrm{r}}$, thus giving a higher stability of the intermediate (expressed by K_1). This consideration implies that for the intermediate, S·α-CD*, the dye is most probably already quite deeply inserted inside the α-CD cavity and close to the final equilibrium position S-α-CD. The structure of the intermediate 3-α-CD*, computed via molecular modeling based on the 2D-NMR data, is in agreement with the proposed mechanism for the first step (Figure 4a) and shows interactions between primary hydroxy groups of the host and the sulfonate of the guest.

Therefore the first step requires (1) an encounter between α-CD and the guest molecule and (2) the desolvation of the sulfonate/sulfonamide group when the guest is initially included in the cavity. (3) At the transition state, interactions can thus exist between the entering group $-SO_3^-$ or $-SO_2NH_2$ and the two not fully coordinated "activated" water molecules which are inside the cavity of the free α-CD.[30] The entrance of the

(30) Saenger, W.; Noltenmeyer, M.; Manor, P. C.; Hingerty, B.; Klar, B. *Bioorg. Chem.* **1976**, *5*, 187.

(31) Gaussian 98 (revision A.6), Frisch, M. J. et al.; Gaussian, Inc.: Pittsburgh, PA, 1998.

guest is concerted with the displacement of these two water molecules into the bulk liquid phase on the narrow rim side of the host. (4) In the intermediate state, S·α-CD*, the sulfonate/sulfonamide group is partially resolvated from the bulk water and hydrogen bonded with the primary hydroxy groups at the narrow rim of the host.

Thermodynamic and activation parameters for the first step are summarized in Table 3. For the series of azo dyes under study, the inclusion process is associated with a negative enthalpy change ($\Delta H_1° \approx -11$ to -35 kJ mol^{-1}) which is largely responsible for the observed stability. The negative entropy change ($\Delta S_1° \approx -43$ to $+15$ J K^{-1} mol^{-1}) is unfavorable as expected with the loss of degree of freedom upon the formation of the complex (note that the only positive $\Delta S_1°$ is related to the most positive $\Delta H_1°$ for dye **2**, which can be attributed to the classical entropy/enthalpy compensation[32] due to a possible small unavoidable systematic error).

The entropy of activation is difficult to interpret conceptually. The negative entropy of the first association step ($\Delta S_{1,f}^{‡} \approx -27$ to -99 J K^{-1} mol^{-1}) contributes unfavorably to the rate of inclusion. This negative value could be rationalized in terms of a substantially frozen motion of the guest molecule in the transition state upon its association with α-CD[33] (translational and rotational freedoms reduced). The contribution of a total freeze of motional freedom of similar guest molecules was estimated to be -209 to -251 J K^{-1} mol^{-1} and is usually partially compensated by positively contributing terms.[34] These may be attributed to the desolvation of the guest entering group, the release of the two water molecules and the conformational change of the α-CD cavity, and the partial collapse of the water cluster around the entering apolar site of the guest molecule. The entropy of activation for the dissociation $\Delta S_{1,r}^{‡}$ is also found to be negative, but its contribution is smaller than $\Delta S_{1,f}^{‡}$ (except for dye **2**). For dye **4**, which enters the cavity via a sulfonamide group, the enthalpies of activation ($\Delta H_{1,f}^{‡}$ and $\Delta H_{1,r}^{‡}$) are larger than those of its analogue, dye **2**, which is included via the sulfonate group. On the other hand, the entropies of activation $\Delta S_{1,f}^{‡}$ and $\Delta S_{1,r}^{‡}$ for the α-CD complex of **4** are much smaller than those of the other dyes; this can be interpreted by a smaller contribution of the desolvation/resolvation around the hydrophobic skeleton reflecting possibly an earlier transition state.

Volume Profile of the First Step. Similar contractions of the reaction volume ($\Delta V_1° \approx -11$ to -4 cm^3 mol^{-1}) are observed for all four dyes between the ground states and the corresponding intermediate states, S·α-CD* (eq 6). Such contractions can be explained by (1) the release of the two not fully coordinated "activated" water molecules from the host cavity upon inclusion of the guest, thus enabling their full hydrogen bonding with the bulk water molecules and leading to a volume contraction, and (2) the enhanced reorganization of the water molecules which were initially positioned at the periphery of the guest molecule upon its insertion in the host cavity, i.e., reduced hydrophobic interactions between the guest skeleton and the bulk water molecules in favor of more contracted apolar interactions between the guest and the hydrophobic α-CD cavity.

In fact, the difference between $-SO_2NH_2$ and $-SO_3^-$ should not be visible in $\Delta V_1°$, since in the intermediate state, the entering group has "partially" passed through the cavity and is probably "partially" resolvated by water molecules from the bulk (see Figure 4).

The volume of activation, $\Delta V^{‡}$, for a substitution reaction[6] is usually considered to be composed of two dominant components: an intrinsic contribution arising from changes in the internuclear distances and angles of the reactants, during bond formation or rupture leading to the transition state, and an electrostrictive contribution that largely arises from changes in the electrostriction of solvent in the second coordination sphere and beyond as distribution of charge and/or dipole changes when the reactants form the transition state.

The currently studied inclusion reactions represent a novel case and cannot be interpreted in a classical manner, i.e., in terms of the intrinsic component, since no covalent bond formation/rupture is involved. In this case, the major contribution to the activation volumes stems from changes in weak interactions, specifically the formation/rupture of hydrogen bonds, and also concurrent structural changes of the flexible host molecule.

The forward activation volumes are all negative and quite similar for guest molecules **1**, **2**, and **3** ($\Delta V_{1,f}^{‡} \approx -24$ to -21 cm^3 mol^{-1}) sharing a sulfonate as an entering group, but smaller in the case of **4** ($\Delta V_{1,f}^{‡} \approx -8$ cm^3 mol^{-1}) with the sulfonamide group. A similar trend applies to the activation volumes, $\Delta V_{1,r}^{‡}$, for the reverse reaction. In the transition state, we assume that the head of the guest molecule is interacting with the inner water molecules of the free host and their complete release is delayed by the primary hydroxy group barrier of the α-CD. A squeezed arrangement develops inside the cavity inducing a large negative activation volume $\Delta V_{1,f}^{‡}$ (see volume profiles in Figure 9). This contraction is reinforced due to the fact that a part of the hydrophobic skeleton of the guest molecule is inside the hydrophobic cavity of the host allowing a better apolar interaction.

The early transition state for dye **4** suggested from the entropy data is readily perceived from the differences in the volumes of activation. In fact $\Delta V_{1,f}^{‡}$ for **4** is the smallest compared to the other dyes. Indeed, an earlier transition state infers a less crowded cavity. This is interpreted in terms of weaker directional interactions of the $-SO_2NH_2$ group with the host inner water molecules compared to the analogous interactions with the $-SO_3^-$ yielding an overall reduced contraction for **4**.

Second Slow Step of the Inclusion. The generalization that has emerged, to date, regarding two-step inclusion reactions of α-CD complexes was mainly composed of a hasty inclusion in the first step and a second step thought to involve slower solvational and conformational changes.[7] Turning to our study, it is clear from Figure 4b that in the second slow step, the sulfonate group of **3** is totally released from the trap previously formed by the primary hydroxy groups of the α-CD and is now solvated by the bulk water molecules. In the final state, the guest is thus further inserted in the host cavity. Possible polar interactions between the tail of the dye and the α-CD larger rim could induce conformational changes of the host cavity thus facilitating such a slipping of the head of the dye out of the α-CD. To support such an interpretation, a close analysis of the kinetic parameters is required.

The forward and reverse rate constants of the second step of the inclusion reaction ($k_{2,f}$ and $k_{2,r}$) for the four dyes follow the same sequence observed for those of the first step. For dyes with the same inserting group $-SO_3^-$, it seems that the more steric and capable of interacting with the α-CD is the tail, the larger is $k_{2,f}$ which is in agreement with our interpretation. Thus the absence of meta substitution in the case of **1** is reflected by its smallest $k_{2,f}$ and K_2 as well as the largest stabilization of its intermediate state, **1**·α-CD*, as expressed by K_1 ($k_{1,r}$ effect).

Switching from $-SO_3^-$ to $-SO_2NH_2$, the forward rate

(32) Rekharsky, M. V.; Inoue, Y. *Chem. Rev.* **1998**, *98*, 1875.
(33) Suzuki, M.; Szejtli, J.; Szente, L. *Carbohydr. Res.* **1989**, *192*, 61.
(34) Tabushi, I.; Kiyosuke, Y.; Sugimoto, T.; Yamamura, K. *J. Am. Chem. Soc.* **1978**, *100*, 916.

constant, $k_{2,f}$, in the case of dye **4** is ca. 30 times faster than that of **2**. We can again suppose that the weaker interaction between the $-SO_2NH_2$ group (Figure 10) with the primary hydroxy groups of the α-CD further facilitates the breaking of this group out of the host cavity.

If the order in K_1 is **1** > **3** > **2** ≥ **4**, that of K_2 is the opposite. The fact that the stabilization of the intermediate S·α-CD* is mainly ruled by $k_{1,r}$ and that $k_{2,f}$ also depends on the steric properties of the non-entering group of the guest reverses the order of K_2. The overall stability ($K_T = K_1 + K_1K_2$) is the highest for the α-CD complex of **1** due to the fact that it is mainly governed by the changes in the K_1 term. Unlike the favorable enthalpy changes for the first inclusion step, the second slow step is associated with positive enthalpy changes ($\Delta H_2° \approx +10$ to $+30$ kJ mol^{-1}), whereas favorable positive entropy changes $\Delta S_2° \approx +50$ to $+100$ J K^{-1} mol^{-1} seem to be largely responsible for the stability of the final product and suggest that conformational changes are taking place (a larger positive $\Delta S_2°$ for dye **1** can be attributed to the classical entropy/enthalpy compensation with an enthalpy change $\Delta H_2°$ close to 30 kJ mol^{-1}). The coupling constant changes ($^3J_{1,2}$) observed for α-CD upon complexation (Table 2) further reflect the conformational changes suggested from entropy data.

Again the interpretation of the entropy of activation is not straightforward. Negative entropy changes for this second step ($\Delta S_{2,f}^{\ddagger} \approx -14$ to -70 J K^{-1} mol^{-1}) reflect as in the first step a frozen mobility of the guest molecules at the second transition state. For the same reason, the entropy of activation for the dissociation $\Delta S_{2,r}^{\ddagger}$ is also negative. Furthermore, the similar and positive enthalpies of activation $\Delta H_{2,f}^{\ddagger}$ and $\Delta H_{2,r}^{\ddagger}$ for the four dyes are most probably related to comparable conformational changes.

Volume Profile of the Second Step. A positive reaction volume is observed for the four dyes with the highest value for guest **1** ($\Delta V_2° \approx +3$ to $+6$ cm^3 mol^{-1} vs $+17$ cm^3 mol^{-1} for **1**). These reaction volumes reflect the breaking of the primary hydroxy group trap around the guest heads as depicted in Figure 4b for dye **3** allowing an expansion of the host cavity. Simultaneously the large α-CD rim is accessible to the tail of the guest molecules. Thus in the case of **1** (no steric hindrance of the tail), an unrestrained deeper encapsulation in the host might induce a larger expansion of the α-CD cavity.

The second transition states for the four dyes are unambiguously associated with volume contractions, $\Delta V_{2,f}^{\ddagger}$, relative to the intermediate states S·α-CD*. Further to the previous interpretation in terms of the formation of hydrogen bonds between the guest tail and the α-CD, a predominant contribution due to an induced flattening of the cavity is required to account for these negative activation volumes. In the case of **1**, the lack of possible hydrogen bond formation of the tail is reflected by a negligible volume $\Delta V_{2,f}^{\ddagger}$ of -2 cm^3 mol^{-1}. On the other hand, a counterbalance appears in the case of the effect of **4** relative to **2** ($\Delta V_{2,f}^{\ddagger}$ of -2.5 vs -16 cm^3 mol^{-1} for **2**), which probably emerges from a partial release of the stiffened host cavity due to an earlier rupture of the primary hydroxy bonds with the sulfonamide head. For the other dyes **2** and **3**, the concurrent interactions of the primary hydroxy groups of the host with the sulfonate head of the guest and the secondary hydroxy groups with the guest tail are partially maintained at the transition state thus reinforcing a substantial contraction of the cavity ($\Delta V_{2,f}^{\ddagger}$ of -12 and -16 cm^3 mol^{-1} for **2** and **3**, respectively).

Conclusion

In light of the volume changes obtained from high-pressure stopped-flow kinetics, coupled to "classical' kinetic investigations and molecular modeling, further mechanistic insight on the α-CD inclusion process is made available. Nevertheless, it is well accepted[7] that a wider range of substrate structures still have to be explored before quantitative generalizations, full mechanistic understanding, and predictive capability are achieved for the inclusion reactions in cyclodextrins. To conclude, this study is a starting point in our project of understanding molecular recognition phenomena using high-pressure techniques.

Supporting Information Available: All stopped-flow kinetic data; 1D ^{1}H NMR titration spectra; tables of the chemical shift changes, $\Delta\delta$ values for the protons of the cyclodextrin and guests; and $\pi-\pi$ stacking NMR and spectrophotometric data (PDF). This material is available free of charge via the Internet at http://pubs.acs.org.

JA993139M